Journal of New Technology and Materials(JNTM)
J. New Technol. Mater.
Vol. 07, N°02 (2017)22-29

OEB Univ. Publish.Co.

Effects of Nickel substitution on crystalline structure and superconducting properties of $YBa_2Cu_3O_{7-\delta}$ ceramics.

Souheila Chamekh[a*], Abderrahmane Bouabellou[a], Yalçin Elerman[b], Melike Kaya[b] and Ilker Dincer[b]

[a] *Thin Films and Interfaces Laboratory, Department of Physics, Faculty of Sciences, University of Constantine 1, Campus Chaab-Erassas, 25000 Constantine, Algeria.*
[b] *Department of Engineering Physics, Faculty of Engineering, Ankara University, 06100 Besevler, Ankara, Turkey*

Corresponding author: email: chamekhsouheila@yahoo.fr

Received date: Jan 27, 2017; revised date: Dec 01, 2017; accepted date: Dec 16, 2017

Abstract

In this study, nickel-substituted $YBa_2(Cu_{1-x}Ni_x)_3O_{7-\delta}$ ($0 \leq x \leq 4$ at.%) superconductor samples were prepared by the conventional solid state reaction method. The effects of Ni substitution on the structure, microstructure, superconducting properties and Raman modes of $YBa_2(Cu_{1-x}Ni_x)_3O_{7-\delta}$ systemshavebeeninvestigated. The Ni-substituted induces a porous, finer grained structure. The energy dispersive X-ray spectroscopy (EDS) analysis confirmed the incorporation of nickel into the grains. RamanspectroscopyshowsthattheincorporationenhancesthedisorderattheCuO_2planes and decreases the oxygen content by the depletion from the CuO chains. The temperature dependent resistivity measurements $\rho(T)$ show a deviation from linearity, due to the opening of a pseudogap. DC susceptibility measurements show that the transition temperature decreases with increasing Ni content.

Keywords: High critical temperature superconductivity; XRD; SEM; Magnetization; Raman spectroscopy.

1. Introduction

High temperature cuprate bulk superconductors REBCO (REBaCuO, RE: Nd, Y, Gd, Sm) can potentially be used for a variety of applications ranging from magnetic bearings, trapped field magnets, energy storage flywheels, levitated transportation systems and superconducting motors because of their high current density and ability of trapping magnetic flux [1].YBCO is one of the most widely studied compound among the high-Tc SC cuprates, due to the simplicity of synthesis procedure by solid-state reaction, the easy availability of the starting powders, and the non-toxicity of the material compared to the other high-Tc superconductors such as Tl and Hg based oxides [2].

The partial substitution in the parent YBCO structure has been investigated intensively in an attempt to clarify or improve the superconducting behavior of this type of superconductors [3-9].It is common that the effect of the rare-earth replacement of Y and Ba in YBCO superconductor has a limited effect on the superconducting transition temperature, with few elements proving to be an interesting exception like praseodymium, On the other hand, the substitution at the Cu site, by the magnetic or nonmagnetic *3d* metals always tends to destroy superconductivity. Unlike the other high T_C perovskite superconductors, the YBCO system has a unique feature: it has two non-equivalent Cu sites viz., the linear-chain Cu(1) in the O(1)-Cu(1)-O(1) units and the planar Cu(2) in the CuO_2 sheets containing O(2) and O(3) [10]. The superconductivity of the system is believed to occur in the Cu(2) planes through hole charge carriers and the oxygen content of Cu(1) chains governs the hole carriers concentration in the CuO_2 planes. Any modification in the CuO_2 planes could strongly influence the electronic structure, the density and mobility of the charge carriers. Previous researches indicate that the cations like Mn, Fe, Co and Al tend to preferentially occupy the Cu(1) chain site. Other cations like Ni, Zn and Li tend to occupy the Cu(2) sites [10-12]. Unlike that, other studies of F. Bridges *et al.* and R.S. Howland *et al.*, cited in Ref [13], based on extended X-ray absorption fine structure (XAFS) analysis and on a differential anomalous X-ray scattering report a random distribution of Ni atoms at both Cu(1) and Cu(2) sites. Furthermore, effects of annealing treatment on Tc of Ni substituted YBCO suggest that the distribution of Ni atoms between chain and plane sites depends on preparation conditions [14]. It is believed that Zn^{2+} ions locally break superconducting pairsproducing a spatial distribution of non-superconductingregions, which are responsiblefor the

increase of the critical current density inmagnetic fields due to the field induced pinning [6].The introduction of magnetic ions in the lattice, as per the Abrikosov–Gor'kov (A–G) pair breaking theory [15], leads to a rapid decrease of $T_C$with increase in the concentration of the magnetic ions due to the interaction of magnetic impurities with the conduction electrons breaking the time-reversal symmetry of the Cooper-pairs [15]. Doping of the magnetic ions like Fe, Co and Ni in the YBCO at the Cu sites induces amagnetic moment and magnetic pair breaking [16].As a result, the substitution with 3d metals suppresses the superconducting transition temperature T_C, which indicates that both non-magnetic and magnetic dopants are equally efficient for the local destruction of antiferromagnetic coupling of Cu atoms on CuO_2 planes [8]. Substitution by the transition metals for Cu sites offers an attractive method of introducing structural disorder. It is common that the electronic properties of high-TcSCcuprates are strongly governed by their crystalline structure. The displacements of ions from their equilibrium positions, as evidenced–proved by- from the vibrational modes, lead to changes in the electronic structure [17].

Raman scattering is an ideal tool for the characterization of high-$T_c$samples. It describes the active phonons and serves to determine disorder, stoichiometry, superstructure, orientation and foreign phases for the characterization of cuprates in the form of single crystals, polycrystalline samples or epitaxial films [18]. The 13 atoms of the orthorhombic unit cell of the superconducting YBCO yield a total of 36 modes, fifteen modes of which are raman-active and twenty one modes are IR-active [19]. In this work, we focus our attention on the raman-active modes which are divided into three symmetry classes: A_{1g}, B_{2g} and B_{3g}. Each class contains five modes which are coupled to the vibrations of Ba, the planar copper atom Cu(2), the planar oxygen$O_2$and O_3, the apical oxygen O_4. The Y lies in an inversion center and thus cannot produce an even raman-active mode [20]. The A_{1g} modes represent the c-axis vibrations of the five atoms, while B_{2g} and B_{3g}modes represent the vibrations in the *a* and *b* direction [17].

In this paper, we present a study of the substitution of the magnetic nickel dopant (Ni) in series of$YBa_2(Cu_{1-x}Ni_x)_3O_{7-\delta}$(YBCNO) $(0 \leq x \leq 4\ at.\%)$samples, and its effects on the crystalline structure, microstructure, magnetic and superconducting properties. With –through-carrying out experiments on raman spectroscopy, we try to understand the interactions of Ni with YBCO system and its effects on the different vibrational modes.

2. Experimental details

The $\boldsymbol{YBa_2(Cu_{1-x}Ni_x)_3O_{7-\delta}}$samples with *x*= 0-4 at.%, were prepared by solid state reaction. Appropriate amounts of high purity of $\boldsymbol{Y_2O_3, BaCO_3, CuO\ and\ NiO}$ were grounded in acetone for 2 hours and heated to 950°C for 30 hours in air. The calcined mixtures were dry-grounded for 1 hour and pelletized with pressure $\boldsymbol{4\ ton/cm^2}$and heated twice in air at$\boldsymbol{950}$ ℃ for 30 hours. Finally, the samples were annealed at $\boldsymbol{500}$ ℃ for 24 hours in oxygen atmosphere. The crystalline structures of our samples were determined by using X-ray diffraction (XRD) operating in Bragg-Brentano geometry (CuKα, Siemens D8-Advance) at room temperature. The cell parameters refinements were performed using the Winplotr and DICVOL06. The microstructure of the samples is observed by using scanning electron microscopy (SEM) (PHILIPS-XL30 ESEM/USA). Raman measurements were performed with 633 nm wavelength excitation by using the Raman microscope (RENISHAW 1000). The magnetic measurements were performed by using a physical properties measurement system (PPMS) under magnetic field 150 Oe between 5 K and 120 K. The temperature dependence of magnetization was measured in zero-field-cooled (ZFC) and field-cooled (FC) modes.

3. Results

3.1. XRD characterization

Figure 1 shows the XRD patterns of the $YBa_2(Cu_{1-x}Ni_x)_3O_{7-\delta}$samples with *x* = 0–4 at.%. The XRD spectra show that the peaks were well matched to the orthorhombic YBCO structure.Theyareattributed to $YBa_2Cu_3O_{7-\delta}$phase ascomparedtoJCPDS 82-2471 file.Appearance of the peaks (003), (004), (005) and (006) in the XRD patterns, with high intensity compared to other peaks, reveal the presence of certain degree of (00l) orientation. It is may be due to stress induced by the thermal cycle, or to the pelletization procedure of the powders.The diffraction peaks of doped samples are shifted to higher 2θ values, which may be due to the stress of first order or to a compressive stress. The peak intensities for YBCO structure are affected by Ni substitution, where the intensities of the peaks are higher for the pure sample as compared with the doped samples. On the contrary, the peaks of the doped samples are larger than the pure one. We conclude that the grain size of the doped samples is smaller than the pure one. The existence of the (013) and (103) lines for all samples confirms that no structural transition from orthorhombic to tetragonal (O-T) crystalline structure. Very small fraction of$BaCuO_2$ $(Y011)$secondary phase appears at 2θ between

28° and 30° up to $x \geq 2\ at.\%$. The peaks of this phase cannot be revealed in the presented patterns because of the chosen scale. The XRD analysis confirms that no Ni containing impurity phase is detected in any sample. These results are in agreement with the one reported by Ref.[10].

As it is common, the full width at half maximum (FWHM) reflects the crystalline quality of the studied samples. Figure 2 shows the variation of full width half maximum (FWHM) (00l) as a function of Ni content. The FWHMs of doped samples are found to be larger than the pure sample, with the exception for (002) and (003) peaks of the 0.5 at.% Ni doped sample. This indicates the existence of defaults in the (00l) direction and thereforethe grain size in these planes is larger for the pure sample than that of the doped ones [21].

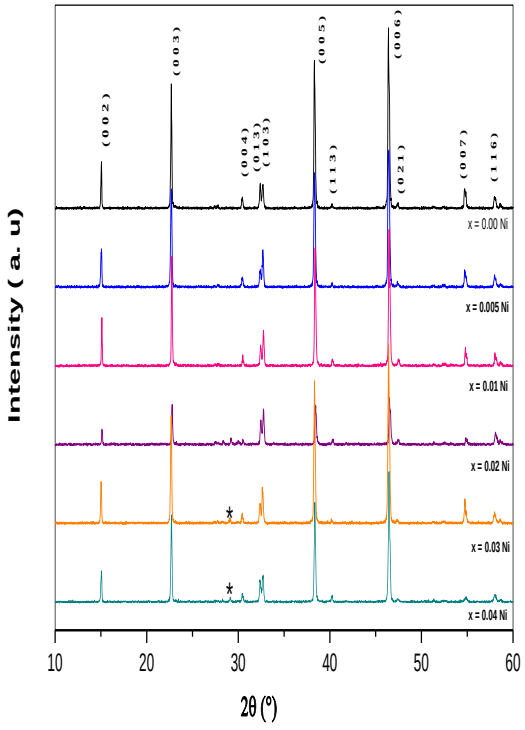

Figure 1: XRD patterns of the $YBa_2(Cu_{1-x}Ni_x)_3O_{7-\delta}$ (x= 0, 0.5, 1, 3, 4 at.%) superconducting samples.

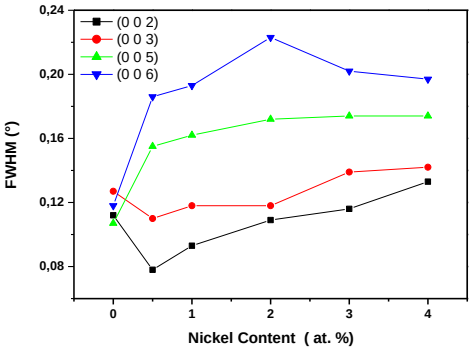

Figure 2: Full width half maximum (FWHM) of (00l) lines as function of nickel content in $YBa_2(Cu_{1-x}Ni_x)_3O_{7-\delta}$ samples.

The grain size for samples is calculated according to Scherrer's formula [22],

$$L = 0.9*\lambda / B*\cos\theta \qquad (1)$$

Where L is the coherence length, θhalf of diffraction angle in degree, λ is the wavelength of X-ray source (Cu-Kα)in nm, and B is the full width at half maximum (FWHM) of the peak. For spherical nanocrystals, the coherence length is related to the diameter d (d=4/3L). The average calculated grain size was found to be in the range of 80 nm and 110 nm.

The variation of lattice parameters *a*, *b* and *c* with nickel content (Fig.3), indicates that *a* is almost constant, *b* and *c* decrease with *x*. The variation change of the lattice parameters supports that Ni is indeed dissolved into the orthorhombic phase. The decrease of *c* parameter confirms the shift of the lines to higher 2θ values as obtained in XRD patterns. The contraction of the crystallographic *c* axis as suggested in [23, 24] could be attributed to the difference in the size of the Ni^{2+} and Cu^{2+}ions($r_{Ni^{2+}} = 0.69$ Å and $r_{Cu^{2+}} = 0.73$ Å) [25], to the loss of oxygen which is known to affect the *c* parameter [26] and can be linked to the reduction in the local Jahn- Teller distortion of the oxygen octahedron aroundCu^{2+}. In cuprate oxides, the Jahn–Teller mode mainly corresponds to an orthorhombic distortion of CuO_2 square in which two Cu-O bonds are elongated and other two shortened [27]. The unit cell dimensions are refined (Table 1) to be *a* = 3.82575 Å, *b* =

3.90718 Å and c = 11.72276 Åfor the pure YBCO phase which is in full agreement with those mentioned in the literature [10, 28].

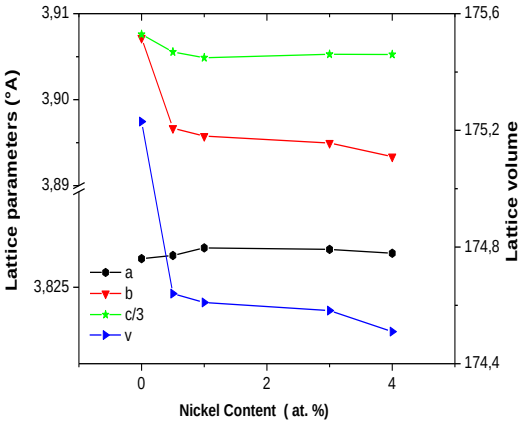

Figure 3: Lattice parameters a, b, c/3 and volume as function of nickel content in $YBa_2(Cu_{1-x}Ni_x)_3O_{7-\delta}$ samples.

Table 1. The lattice parameters *a*, *b* and *c* vs. doping content *x* for $YBa_2(Cu_{1-x}Ni_x)_3O_{7-\delta}$ samples.

Ni content (x at.%)	***a*** (Å)	***b*** (Å)	***c*** (Å)
0.0	3.82575 ± 0.00034	3.90718 ± 0.00022	11.72276 ± 0.00059
0.5	3.82583 ± 0.00036	3.89669 ± 0.00030	11.71666 ±0.00037
1.0	3.82603 ± 0.00054	3.89577 ± 0.00054	11.71463 ± 0.00128
3.0	3.82599 ± 0.00094	3.89496 ± 0.00098	11.71582 ± 0.00042
4.0	3.82589 ± 0.00061	3.89338 ± 0.00064	11.71577 ± 0.00048

The variation of the orthorhombicity (b-a) / (b+a) is plotted in Fig. 4 vs. the Ni content *x*. From this figure, it is easy to note that the orthorhombicity slightly decreases with increasing Ni. The orthorhombic-tetragonal structural transition does not observed in the range 0 ≤ x ≤ 4 %. This result is in agreement with other studies, which show that the O-T structural transition does not take place up to 10% [29] and up to 20% [2]. However, other studies claim that it occurs in the range of 10 ≤ x ≤ 13 %[10]. The orthorhombic strain is lightly dependent on the nickel content *x*, and a small change is in the order of 10^{-3}. We can therefore conclude that the introduction of nickel atoms in YBCOceramics does not affect the orthorhombicity of this superconducting phase.

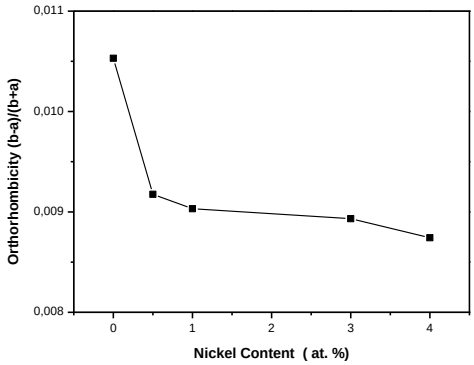

Figure 4: Variation of the orthorhombicity$(b-a)/(b+a)$as function of Nickel content in $YBa_2(Cu_{1-x}Ni_x)_3O_{7-\delta}$

3.2. Surface microstructure

Fig. 5 shows the SEM micrographs of Y123 samples doped with 0, 0.5, 1, 3 and 4% Ni. The observed microstructure exhibits a granular structure with a dominant YBCO phase. It can be seen as the different shape of grains with small fraction of grains having a spherical shape. With the increase of the Ni content the fraction of grains with spherical shape increases. It is also easy to observe the bright grains that the amount increases with Ni content. It is suggested that these grains correspond to the presence of the secondary phase$BaCuO_2$ $(Y011)$. This result is in agreement with that obtained by XRD analysis, and other reported in the work of F.Y. Chuang *et al.* [29]. We can observe another phase which appears between grains (in the grain boundaries, it is indicated by arrows in inset of Fig. 5). The fraction of this phase increases with Ni content and it will be clear to see that it can cover the YBCO grains, as a result the grain size decreases with Ni content. Thus, we conclude that the doping with Ni atoms induces a finer grain with a porous structure. The finer grain would bring more disorder in the grain boundary region, which results an increase of vortex pinning centers and subsequently enhances the critical current [27].

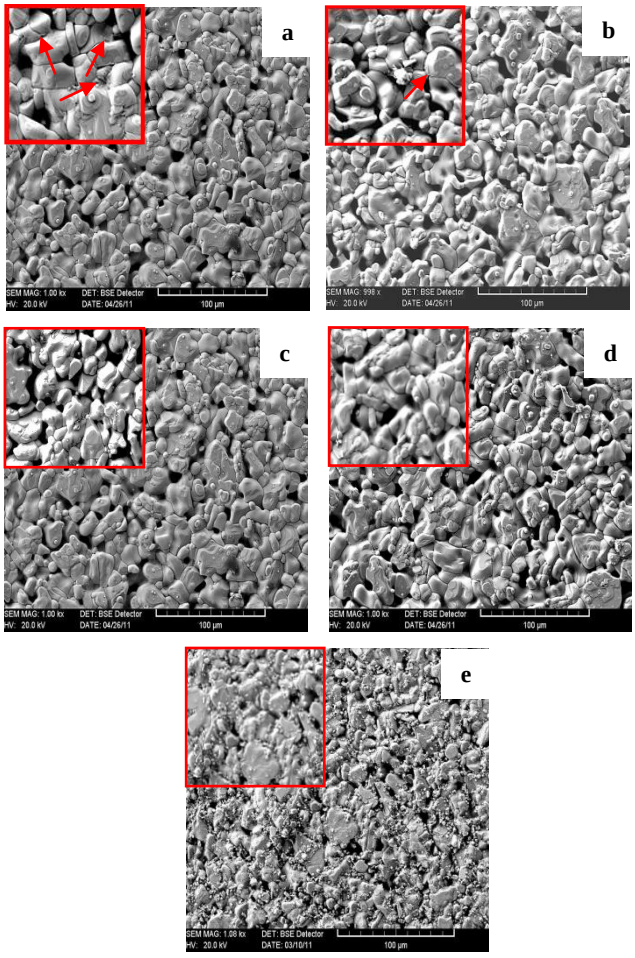

Figure 5 : SEM photographs of samples with formula $Ba_2(Cu_{1-x}Ni_x)_3O_{7-\delta}$: (a) x=0 %,(b) x=0.5%,(c) x=1%, (d) x=3%, (e) x=4%.

The Energy dispersive X-ray spectroscopy (EDS) results of samples with content of Nickel x = 0-4 at.% (Fig.6), confirm the presence of the Y, Ba, Cu, Ni and O elements. A clear signature of the Ni substitution is observed in Cu-site with the doped samples. The EDS analysis confirms the incorporation of nickel into the grains and this result is in consistent with XRD results. The EDS analysis reveals also that the distribution of Ni in the sample is inhomogeneous. It would be important to mention that the EDS is not very good method to estimate the oxygen concentration. We have used Y as reference for the conversion of atomic percentage to the stoichiometry(Table 2).

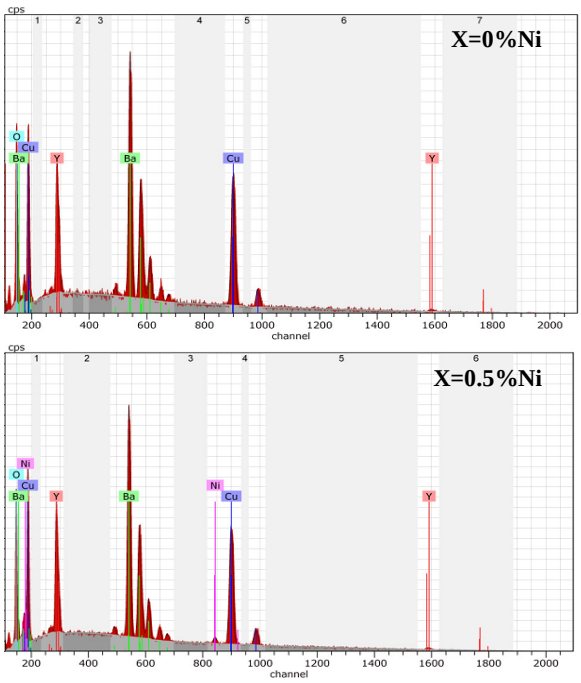

Figure 6: EDS spectrum of samples $YBa_2(Cu_{1-x}Ni_x)_3O_{7-\delta}$with x = 0% and x = 0.5%.

Table 2. Results of EDS analysis in atomic % of samples with content of Ni x = 0.0 % and x = 0.5%.

Sample	Y (%)	Ba (%)	Cu (%)	Ni (%)	O (%)
x= 0.0 %	5.83	10.94	16.11	0	67.13
x= 0.5 %	6.61	10.93	15.48	0.35	66.28

3.3. Raman spectroscopy

Fig. 7 presents the raman spectra recorded for pure and Ni doped YBCO samples. From the modes frequency showed in the Fig. 6(a), it is inferred that YBCO phase is the dominating phase present in our polycrystalline YBCO samples beside small traces of impurity phases. The five Ag raman-active phonons of the YBCO are as follows : the lowest frequency mode involves mainly the vibrations of heaviest barium atom Ba-Ag at$115\ cm^{-1}$ and the copper atoms Cu(2)-Ag at $145cm^{-1}$[1]. The remaining three modes are dominated by the vibrations of O(2), O(3) and the apical oxygen atoms O(4) at $336\ cm^{-1}$, $447\ cm^{-1}$ and $504\ cm^{-1}$ respectively. The first two modes involve the

out-of phasevibrations O(2,3)-Ag and the in-phase vibrations O(2,3)-Ag. Excellent agreement is found for the frequency shifts with theory [17] and with other studies reported in Refs [17-19, 27, 30]. Besides, some additional peaks are seen for all samples, among which three modes are most apparent: $209\ cm^{-1}$ and$574\ cm^{-1}$ are attributed to O4-B_{2g} and O2-B_{2g}. Low intense peak lies at $630\ cm^{-1}$is attributed to the secondary phase $BaCuO_2$ $(Y011)$. The major impurity appears to be YO11, which reflects the inherent instability of YBCO, because this insulating phase is less absorbing than the superconducting phase [19]. Even, small amount of this one can influence the Raman spectra. Another secondary phase is detected, for all samples namely $Y_2BaCuO_7(Y211)$, lying at$180\ cm^{-1}$ and $395\ cm^{-1}$ [31]. It is may-might be that this phase is the unknown phase detected by SEM analysis between grains. These results confirm that the Raman scattering is a very sensitive technique for detecting second phases in the YBCO samples, whereas the XRD analysis could not detect the small amount of the foreign phases.

It is known that the Cu planar sites are the place where the superconductivity occurs and the Ni dopants preferentially occupy Cu(2) sites [5, 6]. For that reason, we must pay attention to the three modes Cu(2)-Ag, out-of phase O(2 ,3)-Ag and in-phase O(2 ,3)-Ag, to depict the effect of Ni doping. The Ba-Ag mode lying at$115\ cm^{-1}$is shifted to lower frequency and has a strong intensity for doped samples, which means the decrease of the mixing between the Ba and the in-plane Cu modes [27]. From Fig. 6, it can be seen that the Cu(2)-Ag mode lying at$150\ cm^{-1}$ is suppressed and broadens with Ni doping. The Ni ions substitute in the planar sites of Cu leads to a decrease in the Cu content. The out-of phase O(2 ,3)-Ag mode is much more intense than that of the undoped sample.

However, the in-phase O(2 ,3)-Ag mode has almost the same character for all samples. The observed softening is consistent with being the result of the Jahn - Teller distortion [27], which couples the electron-phonon to lift the degeneration caused by the Ni substitution. The apical oxygen vibration lying at$504\ cm^{-1}$shifts to lower frequency, the intensity of which in the doped samples is stronger than the pure sample. The frequency of O(4)-Ag mode is known to be associated with the oxygen stoichiometry of the YBCO. The observed softening of this mode is consistent with being the result of the reduction in the **c** parameter of the unit cell with Ni doping in YBCO. It has been established that XRD analysis reveals that the c parameter decreases with increasing Ni content. This mode is well known to be near 480 cm^{-1} for tetragonal YBCO and near $500cm^{-1}$for the orthorhombic form. This result is in agreement with that obtained for XRD analysis, which confirms that no O-T phase transition occurs in the range$0 \leq x \leq 4\%$. From the shift frequency of the O(4)-Ag mode ν and the empirical equation$\delta = 13.58 - 0.027\ \nu$suggested by Huong*et al.* cited in the Ref [32], we can know the variation of the oxygen content, whichdecreases with increasing Ni contents. The all samples are characterized as orthorhombic phase as the oxygen (7-δ) stoichiometry is greater than 6.4.

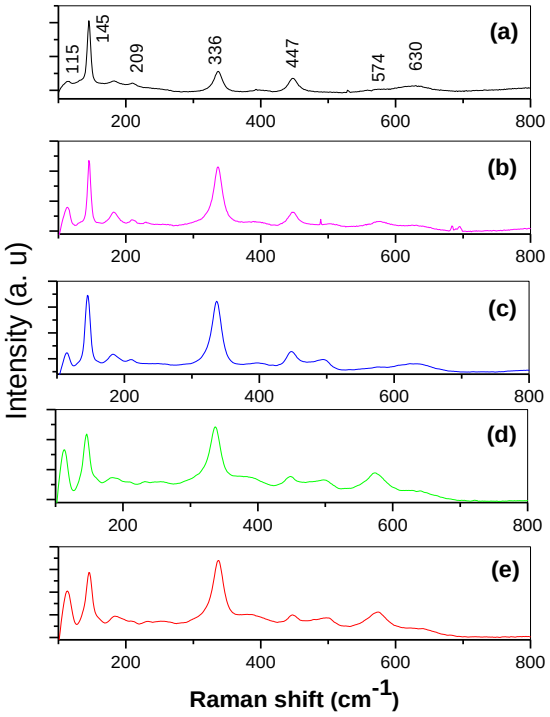

Figure 7: Raman spectra recorded for pure YBCO and variant Ni doped-YBCO samples with formula$Ba_2(Cu_{1-x}Ni_x)_3O_{7-\delta}$: (a) x = 0%,(b) x=0.5%,(c) x=1%, (d) x=3%, (e) x=4%.

3.4.Electrical resistivity

Measurements of different samples with various amounts of Nickel are shown in Fig. 8. As it can be seen, from this figure that the change in the slope $/dT$, for all samples,indicates that these samples are underdoped with charge carriers. The crossover temperature $T^*$is about 190K, and decreases with increasing Ni content. This temperature is may be related to the opening of a normal state pseudo-gap[33], these results are in agreement with other reported by Amira et al, [34] in the system YBCO co-doped with Ca and F. However, an additional heat treatment in flowing oxygen, the resistivity curves do not exhibit this scenario too, then Amira et al, have been suggested that the behavior of resistivity may be related to

defects caused by the quenched such as artfacts, vacancies or impurity phases. The YBCO samples co-doped with Prand Ni donot exhibit the metallic behavior [35]. $\rho\ (o)$is obtained by extrapolating the normal state resistivity to T= 0 K and is related to chemical impurity scattering, lattice defects and hole concentration [36]. $\rho\ (o)$can be expressed as $\rho\ (o) = {m^*}/{ne\tau_0}$, where τ_0 is the scattering diffusion time due to the impurities and m^* is the effective mass of electrons [37]. The increase in$\rho\ (o)$can be easily understood not only by the decrease in the hole concentration but also by the decrease of the relaxation time due to a greater number of defects and heterogeneities created by random distribution of the doping element in samples [37]. It can be seen that T_C^{onset} decreases with increasing x. The decrease in T_C^{onset} temperature is consistent with those reported in [29, 38]. Moreover, the Ni substitution affects the transition widthΔT_C. The lowest value is seen for x=1 at.% of Nickel content. The grains of this sample may be then more homogeneous in comparison with those of other samples [39]. It is suggested that the superconductivity is suppressed by the inter-grain and intra-grain disorders. The lowering in $T_{c.onset}$ is caused by the inter-grain disorder which reduces the effective coupling strength. The inter-grain disorder destroys the phase coherence by reducing the coupling between grains [27]. This result is in agreement with that obtained by The SEM analysis, because the doping with Ni induces a finer grain.

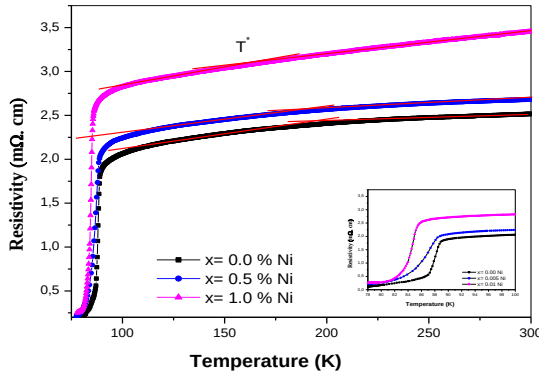

Figure 8: The resistivity dependences on the temperature

3.5. Magnetization measurements

Figure 9 shows the ZFC and FC magnetic curves for the undoped and nickel doped (x = 0.5 at. %) YBCO samples measured with an applied magnetic field of 150 Oe. It is clear that the transition temperature decreases with increasing Ni content. It is may-mightbe due to the change of the carrier density, the disorder of the CuO_2 plane and overall oxygen content [27]. The grains of the doped sample are more homogeneous due to the fact that its transition is slow and wide compared to the pure one. The ZFC and the corresponding FC increase with the content of Ni. The ΔM value at 5 K for the doped sample, $\Delta M = M_{FC} - M_{ZFC}$ where M_{FC} and $M_{ZFC}$are the magnetization values measured in FC and ZFC mode respectively, is larger than the pure one, this means that the grains in the doped sample are more connected [33]. These results are in agreement with that obtained By SEM analysis.It is suggested that the doping with Ni promotes an enhancement of flux trapping capability, because of the increasing in the low temperature value of ΔM [26]. Another feature of these curves may be noticed after beginning of the transition: a change in the slope in the ZFC and FC transitions, this change corresponds to the presence of a secondary superconducting phase. This is in line with SEM observations and XRD spectra which attest the presence of the secondary phase $BaCuO_2$ $(Y011)$. The real superconducting volume of the pure sample is lower than that of the doped one.

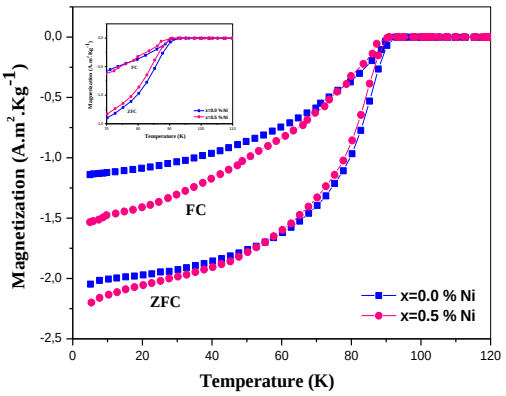

Figure 9: .M(T) curves of pure and nickel (0.5 at.%) doped

4.Conclusion

In conclusion, the effects of Ni substitution on the structural phase transition, superconducting properties and Raman modes of $YBa_2(Cu_{1-x}Ni_x)_3O_{7-\delta}$systems have been investigated. We find that Ni substituted for Cu does not induce orthorhombic-to-tetragonal phase transition in the range 0 ≤ x ≤ 4 %. Scanning electronic micrographs show that the doping with Ni induces a finer grain with a porous structure. The EDS analysis confirmed the incorporation of nickel atoms into the grains. The raman analysis shows that the Ni substitution enhances the disorder of the CuO_2 planes and leads to the decrease of the oxygen. The superconductivity is suppressed by the

inter-grain and intra-grain disorders. The resistivity measurements shows the opening of a normal state pseudogap and the increase of $\rho(o)$ with Ni content, because of the decrease of the hole concentration and the decrease of the relaxation time due to a greater number of the homogeneities in samples. The ZFC and FC curves measured with an applied magnetic field of 150 Oeshow that the doped sample is more homogeneous and the grains are more connected compared to thepure one.

References

[1] P. T. Yang, W. M. Yang, Y. Abula, X. Q. Su, L. L. Zhang, Ceramics International 43 (2017) 3010–3014.
[2] K. Westerholt, M. Arndt, H. Bach and P. Stauche, Physica C. 153-155 (1988) 862-863.
[3] Y. Maeno, M. Kato,Y. Aoki, T. Nojima, T. Fujita, Physica B+C, 148 (1987) 357–359.
[4] J. B. Boyce, F. Briges, T. Claeson, R. S. Howland, T. H. Geballe, M. Nygren, Physica C. 153-155 (1988) 852-853.
[5] D. N. Zheng, A. M. Campbell, J. D. Johnson, J. R. Cooper, F. J. Blunt, A. Porch, P. A. Freeman,Physical Review B. 49(1994) 1417-1426.
[6] L. Shlyk, G. Krabbes, G. Fuchs, G. Stöver, S. Gruss, K. Nenkov, Physica C. 377(2002) 437–444.
[7] L. Zhang, X. F. Sun, X. Chen, H. Zhang, Physica C. 386 (2003) 271–274.
[8] R. Giri, V. P. S. Awana, H. K. Singh, R. S. Tiwari, O. N. Srivastava, A. Gupta, B. V. Kumaraswamy, H. Kishan, Physica C. 419 (2005) 101–108.
[9] F. Ben Azzouz, M. Zouaoui, K. D. Mani, M. Annabi, G. Van Tendeloo, M. Ben Salem, Physica C. 442 (2006) 13–19.
[10] H. Shimizu, T. Kiyama, J. Arai, Physica C. 196(1992) 329-334.
[11] Y. H. Liu, G. C. Che, K. Q. Li, Z. X. Zhao, Z. Q. Kou, N. L. Di, Z. H. Cheng, Physica C. 418 (2005) 63-67.
[12] Y. Zhao, H. K. Liu, X. B. Zhuge, G. Yang, G. Yang, J.A. Xia, Y.Y. He, S.X. Dou, Physica B. 194-196 (1994) 1957-1958.
[13] L. Shlyk, G. Krabbes, G. Fuchs, Physica C. 390(2003) 325–329.
[14] S.Adachi, Y. Itoh, T. Machi, E. Kandyel, S. Tajima, N. Koshizuka, Phys. Rev. B 61 (2000) 4314.
[15] A.A. Abrikosov, L.P. Gor'kov, Sov. Phys. JETP 12 (1961) 1243.
[16] C. Y. Yang, A. R. Moodenbaugh, Y. L. Wang, Youwen Xu, S. M. Heald, D. O. Welch, and M. Suenaga, Physical Review B 42 (1990) 2231-2241.
[17] C. Ambrosch-Draxl, H. Auer, R. Kouba, E. Y. Sherman, P. Knoll, M. Mayer, Physical Review B. 65(2002) 1-9.
[18] S. Hong, H. Cheong, G. Park, Physica C. 470(2010) 383-390.
[19] S. Mozaffari, M. Akhavan, Physica C. 468(2008) 985-990.
[20] C. Thomsen and G. Kaczmarczyk, John Wiley & Sons Ltd, (2002) 1-19.
[21] B. Pignon, C. Autret-Lambert, A. Ruyter, R. Decourt, J. M. Bassat, I. Monot-Laffez, L. Ammor,Physica C. 468 (2008) 865-871.
[22] S. Sapra, D. D. Sarma, Pramana. J. Phys. 65 (2005) 565-570.
[23] G. Xiao, A. Bakhshai, M. Z. Cieplak, Z. Tesanovic, C. L. Chien, Phys. Rev. B 39 (1989) 315-321.
[24] L. Raffo, R. Caciuffo, D. Rinaldi, F. Licci,Supercond. Sci. Technol. 8 (1995) 409.
[25] J. Tonneau, Edition de Boeck université(2000) p9.
[26] S. Attaf, M. F. Mosbah, R. Fittipaldi, D. Zola, S. Pace, A. Vecchione, Physica C. 477(2012) 36-42.
[27] R. Xue, H. Dau, Z. Chen, T. Li, Y. Xue, Materials science and engineering B. 178 (2013) 363-367.
[28] M. A. Rodriguez, A. Navrotsky, F. Licci,Physica C. 329 (2000) 88-94.
[29] F. Y. Chuang, D. J. Sue, C. Y. Sun, Materials Research Bulletin. 30 (1995) 1309-1317.
[30] E. Lee, C. Kim, S. Yoon, S. H. Jang, J. Joo, Journal of the Korean physical society. 53 (2008) 3348-3351.
[31] A. A. Bolzan, G. J. Millar, A. Bhargava, I. D. R. Mackinnon, P. M. Fredericks, Materials Letters B. 28 (1996) 27-32.
[32] R. Xue, Z. Chen, H. Dau, T. Li, Y. Xue, J. Hao, Physica C. 475 (2012) 20-23.
[33] Y. Boudjadja, A. Amira, N. Mahamdioua, A. Saoudel, S. Menassel, A. Varilci, C.Terzioglu, S.P.Altintas, Physica B: Condensed Matter, 505 (2017) 68-73.
[34] A. Amira, M. F. Mosbah, A. Leblanc, P. Molinié, B. Corraze, Phys. Stat. Sol. 7 (2004) 1944-1947.
[35] T. Chakraborty, B. Gahtori, M. A. H. Ahsan, Y. S. Chen, Geetha, Y. K., Kuo, A. Rao, Ch. K. arkar, , S. K. Agrawal, Solid State ommunications, 150 (2010) 454-457.
[36] L. Bouchoucha, F. Ben Azzouz, M. Annabi, M. Zouaoui, M. Ben Salem, Physica C. 470 (2010) 262-268.
[37] Y. Boudjadjaa, A. Amiraa, A. Saoudela, N.l Mahamdiouaa, A. Varilcib, C. Terzioglub, S. P. Altintas,Boletín de la Sociedad Española de Cerámica y Vidrio, 55 (2016) 202-208.
[38] R. K. Singhal, Journal of Alloys and Compounds. 495 (2010) 1–6.
[39] A. Amira, A. Saoudel, Y. Boudjadja, L. Amirouche, N. Mahamdioua, A. Varilci, M. Akdogan,C. Terzioglu, M.F. Mosbah, PhysicaC471(2011) 1621–1626.